Assessing the viability of A_4, S_4, and A_5 flavor symmetries for description of neutrino mixing

S. T. Petcov[1,2,*] and A. V. Titov[3,†]

[1]SISSA/INFN, Via Bonomea 265, 34136 Trieste, Italy
[2]Kavli IPMU (WPI), University of Tokyo, 5-1-5 Kashiwanoha, 277-8583 Kashiwa, Japan
[3]Institute for Particle Physics Phenomenology, Department of Physics, Durham University, South Road, Durham DH1 3LE, United Kingdom

(Received 15 April 2018; published 29 June 2018)

We consider the A_4, S_4, and A_5 discrete lepton flavor symmetries in the case of 3-neutrino mixing, broken down to nontrivial residual symmetries in the charged lepton and neutrino sectors in such a way that at least one of them is a Z_2. Such symmetry breaking patterns lead to predictions for some of the three neutrino mixing angles and/or the leptonic Dirac CP violation phase δ of the neutrino mixing matrix. We assess the viability of these predictions by performing a statistical analysis which uses as an input the latest global data on the neutrino mixing parameters. We find 14 phenomenologically viable cases providing distinct predictions for some of the mixing angles and/or the Dirac phase δ. Employing the current best fit values of the three neutrino mixing angles, we perform a statistical analysis of these cases taking into account the prospective uncertainties in the determination of the mixing angles, planned to be achieved in currently running (Daya Bay) and the next generation (JUNO, T2HK, DUNE) of neutrino oscillation experiments. We find that only six cases would be compatible with these prospective data. We show that this number is likely to be further reduced by a precision measurement of δ.

DOI: 10.1103/PhysRevD.97.115045

I. INTRODUCTION

Flavor is one of the biggest riddles in particle physics. In spite of the tremendous success of the Standard Theory, we do not know why the number of fermion generations is three, what determines the patterns of quark and lepton masses, and what the origins of quark and neutrino mixing are.

Since symmetries proved to be very powerful in guiding the laws of particle physics, it is natural to expect that symmetry might also be a clue to the solution of the flavor problem. For this reason, a variety of *flavor symmetries* has been proposed and explored in the attempts to understand the observed patterns of quark and/or neutrino mixing and of the quark and/or lepton masses. Symmetries described by both continuous groups, including $U(1)$, $SU(2)$, $U(2)$, $SU(3)$, $U(3)$ (see, e.g., [1–6]), and discrete groups, such as S_3, S_4, A_4, T', A_5, as well as the series D_n, $\Delta(3n^2)$, $\Delta(6n^2)$ with $n \in \mathbb{N}$ and Σ groups (see, e.g., [7–9] for reviews and original references) have been considered. Discrete non-Abelian symmetries allow for rotations in the flavor space by fixed (large) angles, which is particularly attractive in view of the fact that two of the three neutrino mixing angles are large [10–12]. Thus, neutrino mixing, as suggested, e.g., in [13], seems to be the appropriate flavor related structure to search for evidence of the existence of an underlying flavor symmetry and therefore, for new physics.

In the framework of the discrete flavor symmetry approach to 3-neutrino mixing[1] on which we will concentrate in the present article, it is assumed that at some high-energy scale there exists a (lepton) flavor symmetry described by a non-Abelian discrete (finite) group. The lepton doublets of the three fermion generations are usually (but not universally) assigned to an irreducible three-dimensional representation of this group, because one aims to unify the three lepton flavors, and this is the case we will consider in the present article. At low energies, the flavor symmetry has necessarily to be broken, because the electron, muon, and tauon charged leptons and the three massive neutrinos are distinct. Generally, the flavor symmetry group G_f is broken in such a way that the charged

*Also at Institute of Nuclear Research and Nuclear Energy, Bulgarian Academy of Sciences, 1784 Sofia, Bulgaria.
†arsenii.titov@durham.ac.uk

[1]For a description of the reference 3-neutrino mixing scheme, see, e.g., [14].

lepton and neutrino mass matrices, M_e and M_ν,[2] or more precisely, the combination $M_e M_e^\dagger$ and M_ν ($M_\nu^\dagger M_\nu$) in the Majorana (Dirac) neutrino case, are left invariant under the action of its Abelian subgroups G_e and G_ν, respectively. These *residual symmetries* constrain the forms of the unitary matrices U_e and U_ν diagonalizing $M_e M_e^\dagger$ and M_ν ($M_\nu^\dagger M_\nu$), and thus of the Pontecorvo, Maki, Nakagawa, Sakata (PMNS) neutrino mixing matrix $U_{\rm PMNS} = U_e^\dagger U_\nu$.

If $G_e = Z_k$, $k > 2$ or $Z_m \times Z_n$, $m, n \geq 2$, and $G_\nu = Z_2 \times Z_2$ ($G_\nu = Z_k$, $k > 2$ or $Z_m \times Z_n$, $m, n \geq 2$) for Majorana (Dirac) neutrinos, the matrices U_e and U_ν are fixed (up to permutations of the columns and diagonal phase matrix on the right). This leads to certain fixed values of the solar, atmospheric, and reactor neutrino mixing angles θ_{12}, θ_{23}, and θ_{13} of the PMNS matrix.[3] Tribimaximal (TBM) mixing [15–18] (see also [19]), characterized by $\theta_{12} = \arcsin(1/\sqrt{3}) \approx 35°$, $\theta_{23} = 45°$, and $\theta_{13} = 0°$, is a well-known example of a symmetry form arising from a specific breaking pattern. Namely, it can be naturally realized by breaking $G_f = S_4$ down to $G_e = Z_3$ and $G_\nu = Z_2 \times Z_2$ [13]. Other widely discussed examples include bimaximal (BM) mixing[4] ($\theta_{12} = \theta_{23} = 45°$, $\theta_{13} = 0°$) [20–22], which can be derived from $G_f = S_4$ [23–25], and golden ratio A (GRA) mixing [$\theta_{12} = \arctan(1/r) \approx 31°$, $\theta_{23} = 45°$, and $\theta_{13} = 0°$, $r = (1+\sqrt{5})/2$ being the golden ratio] [26,27], which can be obtained by breaking $G_f = A_5$ to $G_e = Z_5$ and $G_\nu = Z_2 \times Z_2$ [28,29]. All these highly symmetric mixing patterns, however, were ruled out once θ_{13} was measured and found to have a nonzero value, $\theta_{13} \cong 0.15$. The fact that θ_{13} turned out to have a relatively large value opened up a possibility of establishing the status of Dirac *CP* violation (CPV) in the lepton sector by measuring the Dirac phase δ present in the PMNS matrix. At the same time, it implied, in particular, that the TBM, BM (LC), GRA, and other symmetry forms of the PMNS matrix predicting $\theta_{13} = 0$[5] have to be "perturbed", so that θ_{13}, as well as θ_{12} and θ_{23}, have values compatible with the experimentally determined values. When, for example, the requisite "perturbations" are provided by the matrix U_e and have the simple form of a $U(2)$ transformation in a plane or a product of two $U(2)$ transformations each in a plane, the cosine of the phase δ was shown [34,35] to satisfy a relation by which it is expressed in terms of the three neutrino mixing angles and an angle parameter which takes discrete values depending on the underlying symmetry form [TBM, BM (LC), GRA, GRB, HG] of the PMNS matrix. An analogous relation for $\cos\delta$ arises when, e.g., the TBM symmetry form of $U_{\rm PMNS}$ is "perturbed" on the right by a matrix describing a $U(2)$ transformation in the 1-3 plane [36] or the 2-3 plane [37][6] (see, e.g., [39] for a recent review of the discussed relations between neutrino mixing parameters). The measurement of $\theta_{13} \cong 0.15$ gave also a boost to investigating alternative flavor symmetry breaking patterns in an attempt to explain the special structure of the PMNS matrix.

In [38], all symmetry breaking patterns, i.e., all possible combinations of residual symmetries, which could lead to correlations between some of the three neutrino mixing angles and/or between the neutrino mixing angles and the Dirac CPV phase δ, were considered. Namely, (A) $G_e = Z_2$ and $G_\nu = Z_k$, $k > 2$ or $Z_m \times Z_n$, $m, n \geq 2$; (B) $G_e = Z_k$, $k > 2$ or $Z_m \times Z_n$, $m, n \geq 2$, and $G_\nu = Z_2$; (C) $G_e = Z_2$ and $G_\nu = Z_2$; (D) G_e is fully broken and $G_\nu = Z_k$, $k > 2$ or $Z_m \times Z_n$, $m, n \geq 2$; and (E) $G_e = Z_k$, $k > 2$ or $Z_m \times Z_n$, $m, n \geq 2$, and G_ν is fully broken. For each pattern, relations between the neutrino mixing angles and/or between the neutrino mixing angles and the Dirac CPV phase δ, when present, were derived. Such relations can be present also in the case of the pattern D (E); if due to additional assumptions (e.g., additional symmetries), the otherwise unconstrained unitary matrix U_e (U_ν) is constrained to have the specific form of a matrix of a $U(2)$ transformation in a plane or of the product of two $U(2)$ transformations in two different planes [34,35,38,40,41]. Therefore, the cases of patterns D and E leading to interesting phenomenological predictions are "nonminimal" from the point of view of the symmetries employed (see, e.g., [42–47]), compared to the patterns A, B, and C characterized by nontrivial residual symmetries present in both charged lepton and neutrino sectors, which originate from just one non-Abelian flavor symmetry.

In the present article, we concentrate on the patterns A, B, and C, assuming $G_f = A_4(T')$, S_4, and A_5. When choosing these flavor symmetries, we are guided by minimality: $A_4(T')$, S_4, and A_5 are among smallest (in terms of the number of elements) discrete groups admitting a three-dimensional irreducible representation. In [38], predictions for the mixing angles and $\cos\delta$ have been obtained in the cases of the patterns A, B, and C originating from $G_f = A_4(T')$,[7] S_4, and A_5, using the best fit values of

[2]More specifically, the charged lepton and neutrino mass matrices of the charged lepton and neutrino Majorana (Dirac) mass terms written in left-right and right-left conventions, respectively.

[3]Throughout this article, we use the standard parametrization of the PMNS matrix (see, e.g., [14]).

[4]Bimaximal mixing can also be a consequence of the conservation of the lepton charge $L' = L_e - L_\mu - L_\tau$ (LC) [5], supplemented by $\mu - \tau$ symmetry.

[5]Additional examples of symmetry forms predicting $\theta_{13} = 0$ include the golden ratio B (GRB) form [$\theta_{12} = \arccos(r/2) = 36°$, $\theta_{23} = 45°$] [30,31] and the hexagonal (HG) form ($\theta_{12} = 30°$, $\theta_{23} = 45°$) [32,33].

[6]These two relations can be obtained from the general results derived in [38].

[7]The results obtained in [38] and in the present article for the group A_4 are valid also for T', since when working with the three-dimensional and one-dimensional irreducible representations, T' and A_4 lead to the same results [48].

other (free) mixing angles entering into the correlations of interest. In this work, we perform a statistical analysis of the predictions derived in [38], taking into account (i) the latest global data on the neutrino mixing parameters [49] and (ii) the prospective uncertainties in the determination of the neutrino mixing angles, which are planned to be achieved in the next generation of neutrino oscillation experiments. The results of this analysis clearly demonstrate how phenomenologically viable the considered cases, and hence, the A_4, S_4, and A_5 flavor symmetries, are.

The layout of the remainder of this article is as follows. In Sec. II, we recall the framework and recapitulate the relevant relations between neutrino mixing parameters derived in [38]. In Sec. III, we give a brief description of the discrete groups A_4, S_4, and A_5, emphasizing the features relevant for our analysis. In Sec. IV, we study in detail the predictions for the neutrino mixing angles and the Dirac CPV phase. We perform a statistical analysis of the predictions for $\sin^2\theta_{12}$, $\sin^2\theta_{23}$, and $\cos\delta$ taking into account first the current and then the prospective uncertainties in the determination of the mixing parameters. Finally, we summarize the obtained results and conclude in Sec. V.

II. RESIDUAL SYMMETRY PATTERNS AND CORRELATIONS BETWEEN NEUTRINO MIXING PARAMETERS

In this section, we briefly summarize the results for the patterns A, B, and C obtained in Ref. [38]. We will use these results in Sec. IV to perform a statistical analysis of the predictions for the mixing angles and $\cos\delta$.

Pattern A: $G_e = Z_2$ and $G_\nu = Z_k$, $k > 2$ or $Z_m \times Z_n$, $m, n \geq 2$. The Z_2 residual symmetry in the charged lepton sector fixes the matrix U_e up to a $U(2)$ transformation in the i-j plane. This transformation can be parametrized in terms of a matrix containing one angle and three phases. Two of the three phases can be removed by a redefinition of the charged lepton fields. Therefore, the three neutrino mixing angles and the Dirac phase are expressed in terms of the remaining two free parameters. As a result, correlations between the observables arise. Namely, the considered type of residual symmetries leads to specific relations for $\sin^2\theta_{23}$ and $\cos\delta$, except in one case (case A3, see further) in which $\sin^2\theta_{12}$ and $\sin^2\theta_{13}$ are predicted and δ is not constrained.

Depending on the plane in which the $U(2)$ transformation is performed, one has three cases. The first one, which we denote as A1, corresponds to the transformation in the 1-2 plane and leads to the following expressions:

$$\sin^2\theta_{23} = 1 - \frac{\cos^2\theta_{13}^\circ \cos^2\theta_{23}^\circ}{1-\sin^2\theta_{13}}, \tag{2.1}$$

$$\cos\delta = \frac{\cos^2\theta_{13}(\sin^2\theta_{23}^\circ - \cos^2\theta_{12}) + \cos^2\theta_{13}^\circ\cos^2\theta_{23}^\circ(\cos^2\theta_{12} - \sin^2\theta_{12}\sin^2\theta_{13})}{\sin 2\theta_{12}\sin\theta_{13}|\cos\theta_{13}^\circ\cos\theta_{23}^\circ|(\cos^2\theta_{13} - \cos^2\theta_{13}^\circ\cos^2\theta_{23}^\circ)^{\frac{1}{2}}}, \tag{2.2}$$

where the angles θ_{13}° and θ_{23}° are fixed once the flavor symmetry group G_f and the residual symmetry subgroups G_e and G_ν are specified. In the second case, A2, which corresponds to the free $U(2)$ transformation in the 1-3 plane, one has different relations,

$$\sin^2\theta_{23} = \frac{\sin^2\theta_{23}^\circ}{1-\sin^2\theta_{13}}, \tag{2.3}$$

$$\cos\delta = -\frac{\cos^2\theta_{13}(\cos^2\theta_{12}^\circ\cos^2\theta_{23}^\circ - \cos^2\theta_{12}) + \sin^2\theta_{23}^\circ(\cos^2\theta_{12} - \sin^2\theta_{12}\sin^2\theta_{13})}{\sin 2\theta_{12}\sin\theta_{13}|\sin\theta_{23}^\circ|(\cos^2\theta_{13} - \sin^2\theta_{23}^\circ)^{\frac{1}{2}}}, \tag{2.4}$$

where also the angle θ_{12}° is fixed once G_f, G_e, and G_ν are specified. Finally, case A3 corresponding to the $U(2)$ transformation in the 2-3 plane predicts $\sin^2\theta_{13} = \sin^2\theta_{13}^\circ$ and $\sin^2\theta_{12} = \sin^2\theta_{12}^\circ$, while $\cos\delta$ remains unconstrained.

Pattern B: $G_e = Z_k$, $k > 2$ or $Z_m \times Z_n$, $m, n \geq 2$, and $G_\nu = Z_2$. The residual Z_2 symmetry determines the matrix U_ν up to a $U(2)$ transformation in the i-j plane. For Dirac neutrinos, two of the three phases parametrizing this transformation can be removed by a rephasing of the neutrino fields. For Majorana neutrinos, this is not possible, and these two phases will contribute to the Majorana phases in the PMNS matrix. In either case, they will not enter into the expressions for the mixing angles and the Dirac phase, which depend on the remaining two free parameters (an angle and a phase). Pattern B leads to relations for $\sin^2\theta_{12}$ and $\cos\delta$, again except in one case (case B3, see further) in which $\sin^2\theta_{23}$ and $\sin^2\theta_{13}$ are predicted and δ is not constrained.

Again, depending on the plain of the $U(2)$ transformation, we have three cases. Case B1 corresponding to $(ij) = (13)$ yields

$$\sin^2\theta_{12} = \frac{\sin^2\theta^\circ_{12}}{1-\sin^2\theta_{13}}, \tag{2.5}$$

$$\cos\delta = -\frac{\cos^2\theta_{13}(\cos^2\theta^\circ_{12}\cos^2\theta^\circ_{23} - \cos^2\theta_{23}) + \sin^2\theta^\circ_{12}(\cos^2\theta_{23} - \sin^2\theta_{13}\sin^2\theta_{23})}{\sin 2\theta_{23}\sin\theta_{13}|\sin\theta^\circ_{12}|(\cos^2\theta_{13} - \sin^2\theta^\circ_{12})^{\frac{1}{2}}}, \tag{2.6}$$

where θ°_{12} and θ°_{23} are fixed once the symmetries are specified. In case B2, $(ij) = (23)$, the correlations of interest read

$$\sin^2\theta_{12} = 1 - \frac{\cos^2\theta^\circ_{12}\cos^2\theta^\circ_{13}}{1-\sin^2\theta_{13}}, \tag{2.7}$$

$$\cos\delta = \frac{\cos^2\theta_{13}(\sin^2\theta^\circ_{12} - \cos^2\theta_{23}) + \cos^2\theta^\circ_{12}\cos^2\theta^\circ_{13}(\cos^2\theta_{23} - \sin^2\theta_{13}\sin^2\theta_{23})}{\sin 2\theta_{23}\sin\theta_{13}|\cos\theta^\circ_{12}\cos\theta^\circ_{13}|(\cos^2\theta_{13} - \cos^2\theta^\circ_{12}\cos^2\theta^\circ_{13})^{\frac{1}{2}}}. \tag{2.8}$$

At last, case B3, $(ij) = (12)$, leads to $\sin^2\theta_{13} = \sin^2\theta^\circ_{13}$ and $\sin^2\theta_{23} = \sin^2\theta^\circ_{23}$, and no constraint for $\cos\delta$.

Pattern C: $G_e = Z_2$ and $G_\nu = Z_2$. In this case, both U_e and U_ν are determined up to $U(2)$ transformations in the i-j and k-l planes, respectively. Thus, we have four free parameters (two angles and two phases) in terms of which θ_{ij} and δ are expressed. However, as shown in [38], this number is reduced to three after an appropriate rearrangement of these parameters. As a consequence, a constraint for either $\cos\delta$ or one of $\sin^2\theta_{ij}$ arises.

Depending on the planes in which the free $U(2)$ transformations are performed, we have nine possibilities. We number them as in [38], i.e., cases C1–C9. Four of them lead to expressions for $\cos\delta$, which we summarize below.

$$\text{C1, } (ij,kl) = (12,13)\text{: } \cos\delta = \frac{\sin^2\theta^\circ_{23} - \cos^2\theta_{12}\sin^2\theta_{23} - \cos^2\theta_{23}\sin^2\theta_{12}\sin^2\theta_{13}}{\sin\theta_{13}\sin 2\theta_{23}\sin\theta_{12}\cos\theta_{12}}, \tag{2.9}$$

$$\text{C3, } (ij,kl) = (12,23)\text{: } \cos\delta = \frac{\sin^2\theta_{12}\sin^2\theta_{23} - \sin^2\theta^\circ_{13} + \cos^2\theta_{12}\cos^2\theta_{23}\sin^2\theta_{13}}{\sin\theta_{13}\sin 2\theta_{23}\sin\theta_{12}\cos\theta_{12}}, \tag{2.10}$$

$$\text{C4, } (ij,kl) = (13,23)\text{: } \cos\delta = \frac{\sin^2\theta^\circ_{12} - \cos^2\theta_{23}\sin^2\theta_{12} - \cos^2\theta_{12}\sin^2\theta_{13}\sin^2\theta_{23}}{\sin\theta_{13}\sin 2\theta_{23}\sin\theta_{12}\cos\theta_{12}}, \tag{2.11}$$

$$\text{C8, } (ij,kl) = (13,13)\text{: } \cos\delta = \frac{\cos^2\theta_{12}\cos^2\theta_{23} - \cos^2\theta^\circ_{23} + \sin^2\theta_{12}\sin^2\theta_{23}\sin^2\theta_{13}}{\sin\theta_{13}\sin 2\theta_{23}\sin\theta_{12}\cos\theta_{12}}. \tag{2.12}$$

The neutrino mixing angles in these cases can be treated as free parameters. Other two cases, C5 and C9, yield correlations between $\sin^2\theta_{12}$ and $\sin^2\theta_{13}$. Namely,

$$\text{C5, } (ij,kl) = (23,13)\text{: } \sin^2\theta_{12} = \frac{\sin^2\theta^\circ_{12}}{1-\sin^2\theta_{13}}, \tag{2.13}$$

$$\text{C9, } (ij,kl) = (23,23)\text{: } \sin^2\theta_{12} = \frac{\sin^2\theta^\circ_{12} - \sin^2\theta_{13}}{1-\sin^2\theta_{13}}. \tag{2.14}$$

In cases C2 and C7, instead, there are correlations between $\sin^2\theta_{23}$ and $\sin^2\theta_{13}$,

$$\text{C2, } (ij,kl) = (13,12)\text{: } \sin^2\theta_{23} = \frac{\sin^2\theta^\circ_{23}}{1-\sin^2\theta_{13}}, \tag{2.15}$$

$$\text{C7, } (ij,kl) = (12,12)\text{: } \sin^2\theta_{23} = \frac{\sin^2\theta^\circ_{23} - \sin^2\theta_{13}}{1-\sin^2\theta_{13}}. \tag{2.16}$$

Finally, in case C6, $(ij,kl) = (23,12)$, $\sin^2\theta_{13}$ is predicted to be equal to $\sin^2\theta^\circ_{13}$. In cases C2, C5, C6, C7, and C9, $\cos\delta$ remains unconstrained.

In Sec. IV, we will apply these relations to derive predictions from the A_4, S_4, and A_5 flavor symmetries. We recall that the parameters θ°_{ij} are fixed once the flavor

symmetry group and the residual symmetry subgroups are specified.

III. THE A_4, S_4, AND A_5 SYMMETRIES

The alternating group A_4 is the group of even permutations on four objects. It is isomorphic to the group of rotational symmetries of the regular tetrahedron. All its twelve elements can be expressed in terms of two generators, usually denoted as S and T, which satisfy the following presentation rules:

$$S^2 = T^3 = (ST)^3 = E, \tag{3.1}$$

E being the identity of the group. A_4 possesses four irreducible representations: three 1-dimensional and one 3-dimensional. The eight Abelian subgroups of A_4 amount to three Z_2, four Z_3, and one Klein group K_4 isomorphic to $Z_2 \times Z_2$. The detailed list of them can be found in [50]. All these subgroups can serve as residual symmetries of the charged lepton and neutrino mass matrices.[8] In the case of A_4, we have pairs $(G_e, G_\nu) = (Z_2, Z_3)$ and $(Z_2, Z_2 \times Z_2)$ corresponding to pattern A of residual symmetries, (Z_3, Z_2) and $(Z_2 \times Z_2, Z_2)$ to pattern B, and (Z_2, Z_2) to pattern C.

The symmetric group S_4 is the group of all permutations on four objects. It is isomorphic to the group of rotational symmetries of the cube. It contains A_4 as a subgroup. The 24 elements of S_4 can be generated by two transformations $\tilde{S}$ and $\tilde{T}$ (see, e.g., [7,8]). However, in the context of non-Abelian discrete symmetry approach to neutrino mixing, it often proves convenient to use the three generators S, T, and U, satisfying[9] the following presentation rules:

$$S^2 = T^3 = U^2 = (ST)^3 = (SU)^2 = (TU)^2 = (STU)^4 = E. \tag{3.2}$$

The results from [38] we are going to use in what follows were obtained working with the three generators S, T, and U of S_4. The group admits five irreducible representations: two singlet, one doublet, and two triplet. The list of 20 Abelian subgroups of S_4 consists of nine Z_2, four Z_3, three Z_4, and four $Z_2 \times Z_2$ groups (see, e.g., [50]).

The alternating group A_5 is the group of even permutations on five objects. It is isomorphic to the group of rotational symmetries of the regular icosahedron. Obviously, A_4 is contained in A_5 as a subgroup. The 60 elements of A_5 can be defined in terms of two generators S and T, satisfying[10]

$$S^2 = T^5 = (ST)^3 = E. \tag{3.3}$$

In addition to the two 3-dimensional irreducible representations, the group possesses one singlet, one 4-dimensional, and one 5-dimensional representations. In total, A_5 has 36 Abelian subgroups: 15 Z_2, 10 Z_3, 5 $Z_2 \times Z_2$, and 6 Z_5. The complete list of them can be found in [29].

In [38], all possible pairs of the Abelian subgroups of A_4, S_4, and A_5 listed above, which correspond to patterns A, B, and C discussed in the previous section, have been considered. Using the suitable parametrization of the PMNS matrix in each case, we have obtained the values of the fixed parameters $\sin^2\theta^\circ_{ij}$ relevant for the correlations given in Eqs. (2.1)–(2.16). Finally, employing these correlations and the best fit values of the neutrino mixing angles, we have derived predictions for $\cos\delta$ and $\sin^2\theta_{ij}$. They are summarized in Tables 9–11 in [38].

In the next section, we first update the predictions for $\cos\delta$ and $\sin^2\theta_{ij}$ using the best fit values of the mixing angles obtained in the latest global analysis of neutrino oscillation data [49]. Secondly, and most importantly, we perform a statistical analysis of the predictions, taking into account (i) the latest global data on the neutrino mixing parameters [49] and (ii) the prospective uncertainties in the determination of the mixing angles, which are planned to be achieved in the next generation of neutrino oscillation experiments. As we will see, the results of our analysis clearly demonstrate how phenomenologically viable the cases under consideration are at the moment and what the perspective for testing them is.

IV. PREDICTIONS FOR THE MIXING ANGLES AND THE DIRAC CPV PHASE

Before proceeding to the numerical results, we would like to make a comment on the number of possible cases we have, since *a priori* this number is large, and one could be surprised by a relatively small number of *viable* cases we find and present in what follows.

Let us consider as an example $G_f = A_4$. First, we examine the residual symmetries G_e and G_ν, which lead to fully specified mixing patterns. There are four such types of pairs (G_e, G_ν). We comment on each of them below.

(i) $(G_e, G_\nu) = (Z_2 \times Z_2, Z_2 \times Z_2)$. In this case, the matrices U_e and U_ν are the same (up to permutations of the columns and diagonal phase matrices on the right). Therefore, the PMNS matrix is given by the unit matrix up to permutations of rows and columns and possible Majorana phases. This case is clearly nonviable.

(ii) $(G_e, G_\nu) = (Z_3, Z_2 \times Z_2)$. There are four such pairs in the case of $G_f = A_4$. All of them are conjugate to each other. As is well known, two pairs of residual symmetries, which are conjugate to each other under an element of G_f, lead to the same PMNS matrix

[8] We recall that in the case of Majorana neutrinos the residual symmetry G_ν can be either Z_2 or $Z_2 \times Z_2$.

[9] This presentation of S_4 is convenient, because S and T alone generate the A_4 subgroup of S_4.

[10] We note that the generators S and T of A_5 are different from the corresponding generators of A_4 and S_4 denoted by the same letters.

(see, e.g., [51,52]). Thus, it is enough to consider only one of them. The resulting PMNS matrix is fixed up to permutations of rows and columns, but is not viable (see, e.g., [52]).

(iii) $(G_e, G_\nu) = (Z_2 \times Z_2, Z_3)$. Again, four possible pairs are conjugate to each other and lead to the same PMNS fixed up to permutations of rows and columns. This case is not consistent with the data either.

(iv) $(G_e, G_\nu) = (Z_3, Z_3)$. The 16 possible $(Z_3^{g_e}, Z_3^{g_\nu})$ pairs, g_e and g_ν being the generating elements of the $Z_3^{g_e}$ and $Z_3^{g_\nu}$ subgroups, respectively, fall into two groups. There are four pairs with $g_e = g_\nu$ and twelve pairs with $g_e \neq g_\nu$. The former four are conjugate to each other and lead to the same PMNS matrix, which corresponds to the unit matrix up to permutations of rows and columns. The latter twelve are also related to each other by a similarity transformation, thus leading to the same PMNS matrix fixed, as always, up to permutations of rows and columns. This pattern is not viable as well.

Secondly, considering patterns A, B, and C of the residual symmetries G_e and G_ν, which do not lead to fully specified $U_{\rm PMNS}$, we have five possibilities.

(i) $(G_e, G_\nu) = (Z_2, Z_2 \times Z_2)$. There are three such pairs for $G_f = A_4$, all of them being conjugate to each other. Thus, it is enough to consider only one of them. However, in the case of A_4, any Z_2 is a subgroup of the $Z_2 \times Z_2$. As shown in [38], $(G_e, G_\nu) = (Z_2^{g_e}, Z_2^{g_\nu} \times Z_2)$ and $(G_e, G_\nu) = (Z_2^{g_e} \times Z_2, Z_2^{g_\nu})$ with g_e and g_ν belonging to the same $Z_2 \times Z_2$ subgroup of G_f, lead to some entries of $U_{\rm PMNS}$ being zero, which is ruled out by the data [49].

(ii) $(G_e, G_\nu) = (Z_2, Z_3)$. One can demonstrate that the twelve possible pairs are all conjugate to each other, and thus, they predict the same PMNS matrix. The latter is defined up to a free $U(2)$ transformation applied from the left in the i-j plane (three possibilities) as explained in Sec. II and up to permutations of columns.

(iii) $(G_e, G_\nu) = (Z_2 \times Z_2, Z_2)$. There are three such pairs, all of them being related to each other by a similarity transformation. The same argument as for $(G_e, G_\nu) = (Z_2, Z_2 \times Z_2)$ works in this case. The resulting PMNS matrix is not viable, because it contains zero entries.

(iv) $(G_e, G_\nu) = (Z_3, Z_2)$. The twelve possible pairs are all conjugate to each other, and thus, they predict the same PMNS matrix. It is defined up to a free $U(2)$ transformation applied from the right in the i-j plane (three possibilities) as explained in Sec. II and up to permutations of columns. As we will see, the case of the transformation in the 1-3 plane is the only case consistent with the data.

TABLE I. The best fit values and 3σ ranges of the neutrino mixing parameters obtained in the latest global analysis of neutrino oscillation data [49]. NO (IO) stands for normal (inverted) ordering of the neutrino mass spectrum.

Parameter	Best fit	3σ range
$\sin^2\theta_{12}$	0.307	0.272–0.346
$\sin^2\theta_{23}$ (NO)	0.538	0.418–0.613
$\sin^2\theta_{23}$ (IO)	0.554	0.435–0.616
$\sin^2\theta_{13}$ (NO)	0.02206	0.01981–0.02436
$\sin^2\theta_{13}$ (IO)	0.02227	0.02006–0.02452
δ [°] (NO)	234	144–374
δ [°] (IO)	278	192–354

(v) $(G_e, G_\nu) = (Z_2, Z_2)$. The nine possible $(Z_2^{g_e}, Z_2^{g_\nu})$ pairs can be partitioned into two equivalent classes. The first class contains three pairs with $g_e = g_\nu$, which are conjugate to each other. They lead to the same PMNS matrix with zero entries (see, e.g., [38,53]). The second class consists of six pairs with $g_e \neq g_\nu$, all of them being related to each other by a similarity transformation. Since $g_e, g_\nu \in Z_2 \times Z_2 \subset A_4$, the resulting PMNS matrix contains a zero entry in this case as well [38,53]. Therefore, the considered pattern is not viable.

Thus, the total number of cases is 64 (up to permutations of the rows and columns of the predicted neutrino mixing matrix). Of these, only eight lead to distinct predictions for $U_{\rm PMNS}$, while only five cases *a priori* can be phenomenologically viable.[11] Similar analyses can be performed for the S_4 and A_5 symmetries.

In our further analysis, we require that all three mixing angles lie simultaneously in their respective 3σ ranges, and that the constraint for $\cos\delta$, whenever present, leads to $|\cos\delta| \leq 1$ (see further). Thus, the number of the remaining cases gets further reduced by these requirements.

A. Analysis with best fit values

In this section, we use the best fit values of the mixing angles found in the latest global analysis [49] to update the numerical predictions for $\cos\delta$ and $\sin^2\theta_{ij}$ obtained in [38]. For convenience, we present the current best fit values of $\sin^2\theta_{ij}$ and δ along with their respective 3σ ranges in Table I.

In the case of $G_f = A_4$, there is *only one* phenomenologically viable case. Namely, this is case B1 with $(G_e, G_\nu) = (Z_3, Z_2)$, which yields $(\sin^2\theta_{12}^\circ, \sin^2\theta_{23}^\circ) = (1/3, 1/2)$ and corresponds to the TBM mixing matrix corrected from the right by a $U(2)$ transformation in the 1-3 plane. Making use of Eqs. (2.5) and (2.6) and the current best fit values of the mixing angles for the NO neutrino

[11] By "*a priori*" we mean that they lead to $U_{\rm PMNS}$ without zero entries.

mass spectrum, we find the predictions summarized in Table II. In the next sections, we will investigate in detail how these predictions modify, if one takes into account the uncertainties in the determination of the neutrino mixing parameters.

In the case of $G_f = S_4$, the number of viable cases is larger; namely, there are eight viable cases. We summarize them in Table III. In the cases marked with an asterisk, the use of the best fit values of the mixing angles leads to unphysical values of $\cos\delta$, i.e., $|\cos\delta| > 1$, which reflects the fact that these cases cannot provide a good description of the best fit values of all three mixing angles simultaneously. However, the physical values of $\cos\delta$ can be obtained in these cases fixing two angles to their best fit values and varying the third one in its 3σ range.

Finally, for $G_f = A_5$, requiring the compatibility with the data in the way explained above, we find 13 viable cases. They are presented in Table IV. The exact algebraic forms of the irrational values of $\sin^2\theta^\circ_{ij}$ in Table IV have been found in [38]. They are related to the golden ratio $r = (1+\sqrt{5})/2$ as follows: $2/(4r^2 - r) \approx 0.226$, $r/(6r-6) \approx 0.436$, $1/(2+r) \approx 0.276$, $1/(4r^2) \approx 0.095$, $1/(3+3r) \approx 0.127$, and $(3-r)/4 \approx 0.345$.

TABLE II. The only viable case for $G_f = A_4$. The values of $\cos\delta$ and $\sin^2\theta_{12}$ are obtained using the best fit values of $\sin^2\theta_{13}$ and $\sin^2\theta_{23}$ for NO.

(G_e, G_ν)	Case	$\sin^2\theta^\circ_{ij}$	$\cos\delta$	$\sin^2\theta_{ij}$
(Z_3, Z_2)	B1	$(\sin^2\theta^\circ_{12}, \sin^2\theta^\circ_{23}) = (1/3, 1/2)$	−0.353	$\sin^2\theta_{12} = 0.341$

TABLE III. The viable cases for $G_f = S_4$. The values of $\cos\delta$ and $\sin^2\theta_{12}$/ $\sin^2\theta_{23}$ are obtained using the best fit values of the relevant (not fixed) mixing angles for NO. In the cases marked with an asterisk, physical values of $\cos\delta$ cannot be obtained employing the best fit values of the mixing angles, but they are achievable fixing two angles to their best fit values and varying the third one in its 3σ range.

(G_e, G_ν)	Case	$\sin^2\theta^\circ_{ij}$	$\cos\delta$	$\sin^2\theta_{ij}$
(Z_3, Z_2)	B1	$(\sin^2\theta^\circ_{12}, \sin^2\theta^\circ_{23}) = (1/3, 1/2)$	−0.353	$\sin^2\theta_{12} = 0.341$
	$B2S_4$	$(\sin^2\theta^\circ_{12}, \sin^2\theta^\circ_{13}) = (1/6, 1/5)$	0.167	$\sin^2\theta_{12} = 0.318$
(Z_2, Z_2)	C1	$\sin^2\theta^\circ_{23} = 1/4$	-1^*	not fixed
	$C2S_4$	$\sin^2\theta^\circ_{23} = 1/2$	not fixed	$\sin^2\theta_{23} = 0.511$
	C3	$\sin^2\theta^\circ_{13} = 1/4$	-1^*	not fixed
	C4	$\sin^2\theta^\circ_{12} = 1/4$	1^*	not fixed
	$C7S_4$	$\sin^2\theta^\circ_{23} = 1/2$	not fixed	$\sin^2\theta_{23} = 0.489$
	C8	$\sin^2\theta^\circ_{23} = 3/4$	1^*	not fixed

TABLE IV. The same as in Table III, but for $G_f = A_5$.

(G_e, G_ν)	Case	$\sin^2\theta^\circ_{ij}$	$\cos\delta$	$\sin^2\theta_{ij}$
(Z_2, Z_3)	$A1A_5$	$(\sin^2\theta^\circ_{13}, \sin^2\theta^\circ_{23}) = (0.226, 0.436)$	0.727	$\sin^2\theta_{23} = 0.554$
	$A2A_5$	$(\sin^2\theta^\circ_{12}, \sin^2\theta^\circ_{23}) = (0.226, 0.436)$	−0.727	$\sin^2\theta_{23} = 0.446$
(Z_3, Z_2)	B1	$(\sin^2\theta^\circ_{12}, \sin^2\theta^\circ_{23}) = (1/3, 1/2)$	−0.353	$\sin^2\theta_{12} = 0.341$
(Z_5, Z_2)	$B1A_5$	$(\sin^2\theta^\circ_{12}, \sin^2\theta^\circ_{23}) = (0.276, 1/2)$	−0.405	$\sin^2\theta_{12} = 0.283$
$(Z_2 \times Z_2, Z_2)$	$B2A_5$	$(\sin^2\theta^\circ_{12}, \sin^2\theta^\circ_{13}) = (0.095, 0.276)$	−0.936	$\sin^2\theta_{12} = 0.331$
	$B2A_5II$	$(\sin^2\theta^\circ_{12}, \sin^2\theta^\circ_{13}) = (1/4, 0.127)$	1^*	$\sin^2\theta_{12} = 0.331$
(Z_2, Z_2)	C1	$\sin^2\theta^\circ_{23} = 1/4$	-1^*	not fixed
	$C3A_5$	$\sin^2\theta^\circ_{13} = 0.095$	1^*	not fixed
	C3	$\sin^2\theta^\circ_{13} = 1/4$	-1^*	not fixed
	$C4A_5$	$\sin^2\theta^\circ_{12} = 0.095$	−0.799	not fixed
	C4	$\sin^2\theta^\circ_{12} = 1/4$	1^*	not fixed
	C8	$\sin^2\theta^\circ_{23} = 3/4$	1^*	not fixed
	$C9A_5$	$\sin^2\theta^\circ_{12} = 0.345$	not fixed	$\sin^2\theta_{12} = 0.331$

We note that case B1 is common to all the three flavor symmetry groups A_4, S_4, and A_5, while cases C1, C3, C4, and C8 are shared by S_4 and A_5. Thus, we have 16 cases in total, which lead to different predictions for $\sin^2\theta_{12}$ or $\sin^2\theta_{23}$ and/or $\cos\delta$. As we will see in the next section performing a statistical analysis of these predictions, two cases, namely, C4 and B2A_5II, are globally disfavored at more than 3σ confidence level. Thus, the total number of phenomenologically viable cases reduces to 14.

B. Statistical analysis: Current data

It is important to perform a statistical analysis of the predictions for the mixing parameters discussed in the previous section in order to have a clear picture of their compatibility with the current global neutrino oscillation data as well as to assess the prospects for their future tests. To this aim, we will follow the method of constructing an approximate global likelihood function, which was successfully applied in [35,40,41] (see also [54]). We briefly describe this method below.

The NuFIT Collaboration performing a global analysis of neutrino oscillation data provides one-dimensional χ^2 projections for $\sin^2\theta_{ij}$ and δ [49]. We denote them as $\chi^2_i(x_i)$, $i = 1,2,3,4$, where x_i are components of $\vec{x} = (\sin^2\theta_{12}, \sin^2\theta_{13}, \sin^2\theta_{23}, \delta)$. Using these projections, we construct an approximate global χ^2 function as

$$\chi^2(\vec{x}) = \sum_{i=1}^{4} \chi^2_i(x_i). \tag{4.1}$$

For each model (B1, B2S_4, C1, etc.), the "standard" mixing parameters composing vector $\vec{x}$ are not independent, but are related to each other via the expressions summarized in Sec. II. Thus, in order to obtain a one-dimensional χ^2 function for the observable α of interest ($\alpha = \sin^2\theta_{12}$, $\sin^2\theta_{23}$, or $\cos\delta$), we need to minimize the global $\chi^2(\vec{x})$ for each value of α taking into account the correlations between the mixing parameters x_i, i.e.,

$$\chi^2(\alpha) = \min\left[\chi^2(\vec{x})|_{\substack{\text{constraints}\\ \alpha=\text{const}}}\right]. \tag{4.2}$$

Finally, we define the global likelihood function as

$$L(\alpha) = \exp\left(-\frac{\chi^2(\alpha)}{2}\right). \tag{4.3}$$

Cases predicting $\sin^2\theta_{12}$. As can be seen from Tables II–IV, there are six different cases which lead to predictions for $\sin^2\theta_{12}$. Namely, they read B1, B2S_4, B1A_5, B2A_5, B2A_5II, and C9A_5. We have performed statistical analysis of the predictions for $\sin^2\theta_{12}$ as described above. In Fig. 1, we present the obtained likelihood functions. In the left (right) panel, we have used as an input the one-dimensional projections $\chi^2_i(x_i)$ for NO (IO). We would like to note that according to [49], there is an overall preference for NO over IO of $\Delta\chi^2 = 4.14$. However, we take a conservative approach and treat both orderings on equal grounds in our analysis.

Five cases presented in Fig. 1 lead to very sharp predictions for $\sin^2\theta_{12}$. The corresponding likelihood profiles are very narrow because their widths are determined by the small uncertainty on $\sin^2\theta_{13}$ as can be understood from Eqs. (2.5), (2.7), and (2.14). Case B1 is compatible with the global data at 3σ. Cases B1A_5 and B2A_5 almost touch the 2σ line for NO and are within 3σ for IO. C9A_5 is compatible with the data at 2σ. Finally, B2S_4 is the case which is favored most by the present data, being compatible with them at 1.5σ for NO and 1σ for IO. We find that case B2A_5II is globally disfavored at more than 3σ, the value of χ^2 in the minimum, χ^2_{min}, being equal to

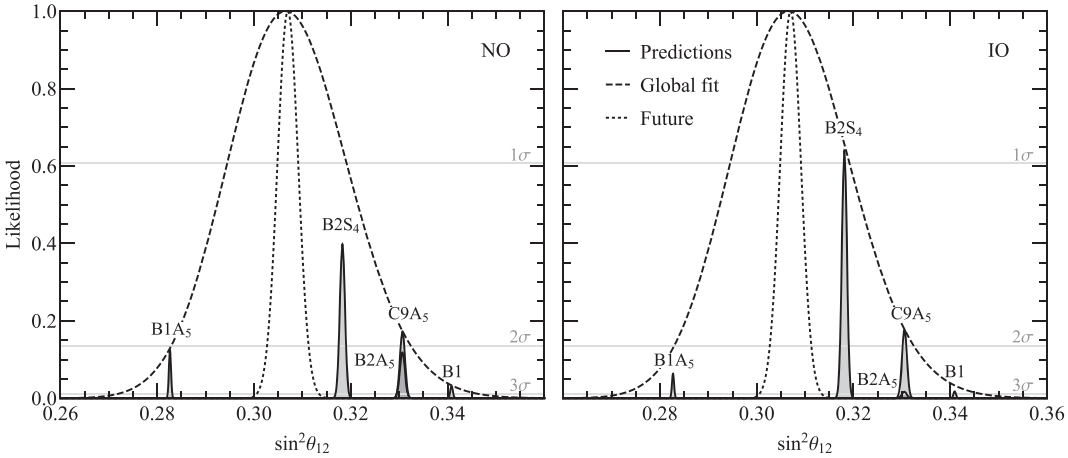

FIG. 1. Predictions for $\sin^2\theta_{12}$ obtained using the current global data on the neutrino mixing parameters. "Future" (the dotted line) refers to the scenario with $\sin^2\theta^{\text{bf}}_{12} = 0.307$ (current best fit value) and the relative 1σ uncertainty of 0.7% expected from the JUNO experiment. See text for further details.

9.9 (13.7) for NO (IO). Thus, we do not present this case in Fig. 1.

The dashed line corresponds to the likelihood for $\sin^2\theta_{12}$ extracted from the global analysis, i.e., calculated substituting the one-dimensional projection $\chi^2_1(\sin^2\theta_{12})$ in Eq. (4.3) in place of $\chi^2(\alpha)$. It is clear from the way in which the likelihood function is constructed that none of the predicted likelihood profiles can go beyond the dashed line. The dotted line instead represents the prospective precision on $\sin^2\theta_{12}$ of 0.7%, which is planned to be achieved by the medium-baseline reactor oscillation experiment JUNO [55]. More precisely, the corresponding likelihood is calculated using Eq. (4.3) with a replacement of $\chi^2(\alpha)$ by

$$\chi^2_{1,\text{future}}(\sin^2\theta_{12}) = \left(\frac{\sin^2\theta_{12} - \sin^2\theta^{\text{bf}}_{12}}{\sigma(\sin^2\theta_{12})}\right)^2, \quad (4.4)$$

where $\sin^2\theta^{\text{bf}}_{12} = 0.307$ is the current best fit value of $\sin^2\theta_{12}$, and $\sigma(\sin^2\theta_{12}) = 0.007 \times \sin^2\theta^{\text{bf}}_{12}$ is the prospective 1σ uncertainty in its determination. Thus, we make an assumption that the best fit value of $\sin^2\theta_{12}$ will not change in the future. If it is indeed the case, then, as is clear from Fig. 1, all five models, B1, B2S_4, B1A_5, B2A_5, and C9A_5, will be ruled out by the JUNO measurement of $\sin^2\theta_{12}$. If, however, the best fit value changed coinciding, e.g., with that of case B1A_5 (B2S_4), cases B2S_4 (B1A_5), B2A_5, C9A_5, and B1 would be ruled out.

Cases predicting $\sin^2\theta_{23}$. There are four cases leading to predictions for $\sin^2\theta_{23}$: C2S_4, C7S_4, A1A_5, and A2A_5. We show the corresponding likelihood functions in Fig. 2. Since, in these cases $\sin^2\theta_{23}$ is determined by $\sin^2\theta_{13}$, see Eqs. (2.1), (2.3), (2.15), and (2.16), the predicted likelihood profiles are very narrow. Cases C2S_4 and C7S_4 are well compatible with the data for NO (at less than 1σ) and with the data for IO (at around 1.5σ). What concerns cases A1A_5 and A2A_5, they reconcile with the data for NO at 2σ. For IO, A1A_5 is within 1.5σ, while A2A_5 is disfavored at more than 3σ ($\chi^2_{\text{min}} = 10.1$). This is why this case is not present in the right panel of Fig. 2.

Similarly to the previous figure, the dashed line corresponds to the global fit likelihood obtained from the one-dimensional projection $\chi^2_3(\sin^2\theta_{23})$. The dotted line indicates the prospective precision on $\sin^2\theta_{23}$ of 3%. It is worth noting that the error on $\sin^2\theta_{23}$, which can be reached in the next generation of long-baseline (LBL) neutrino oscillation experiments like DUNE [56,57] and T2HK [58,59], depends on the true value of this parameter. As can be seen, e.g., from Fig. 10 in [60], in the case of T2HK, this error varies from 1% for the true values of $\sin^2\theta_{23}$ on the boundaries of its 3σ range to approximately 6% for $\sin^2\theta_{23} = 0.5$. For the current best fit value of $\sin^2\theta_{23} = 0.538$ (for NO), the expected uncertainty does not exceed 3%, and we take it as a benchmark value. The likelihood corresponding to the dotted line is calculated using

$$\chi^2_{3,\text{future}}(\sin^2\theta_{23}) = \left(\frac{\sin^2\theta_{23} - \sin^2\theta^{\text{bf}}_{23}}{\sigma(\sin^2\theta_{23})}\right)^2, \quad (4.5)$$

where $\sin^2\theta^{\text{bf}}_{23} = 0.538(0.554)$ is the current best fit value of $\sin^2\theta_{23}$ for NO (IO), and $\sigma(\sin^2\theta_{23}) = 0.03 \times \sin^2\theta^{\text{bf}}_{23}$ is the prospective 1σ uncertainty. If the current best fit value does not change in the future, case A2A_5 will be ruled out, while case C7S_4 will be disfavored at 3σ. However, if the best fit value changed, e.g., to 0.5 for both NO and IO spectra, cases C2S_4 and C7S_4 would be phenomenologically viable, while cases A1A_5 and A2A_5 would be disfavored at 3σ (see Fig. 2).

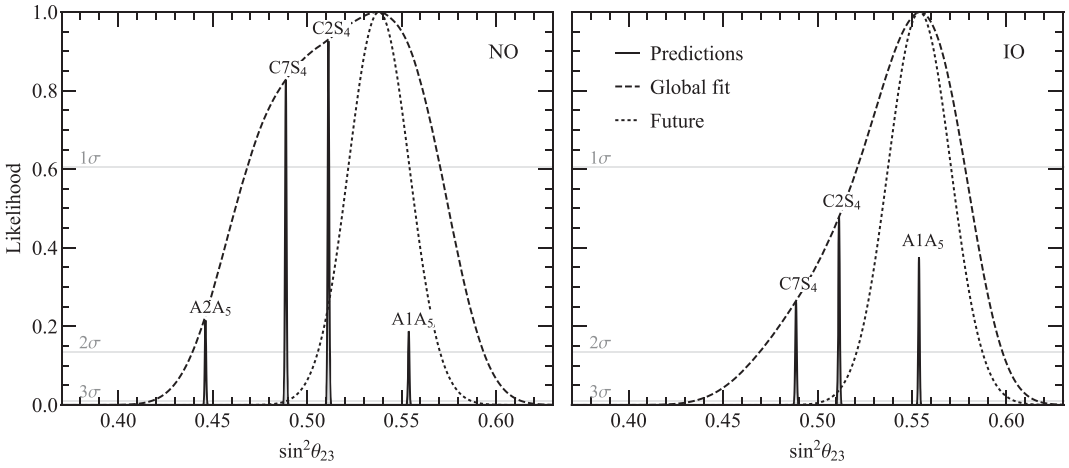

FIG. 2. Predictions for $\sin^2\theta_{23}$ obtained using the current global data on the neutrino mixing parameters. "Future" (the dotted line) refers to the scenario with $\sin^2\theta^{\text{bf}}_{23} = 0.538(0.554)$ for NO (IO) (current best fit values) and the relative 1σ uncertainty of 3% expected from DUNE and T2HK. See text for further details.

Cases predicting $\cos\delta$. As has been discussed in Sec. II and can be seen from Tables II–IV, cases A and B of interest lead not only to predictions for $\sin^2\theta_{23}$ and $\sin^2\theta_{12}$, respectively, but also to predictions for $\cos\delta$. Using Eqs. (2.1)–(2.8), we have performed statistical analysis of these predictions. The obtained results are summarized in Fig. 3. We find that the predictions for $\cos\delta$ in cases B are very sensitive to the value of θ_{23} [cf. Eqs. (2.6) and (2.8)], which is determined with a larger uncertainty than θ_{12} and θ_{13}. This results in quite broad likelihood profiles. For cases A, the uncertainty in predicting $\cos\delta$ from Eqs. (2.2) and (2.4) is driven by the uncertainty on $\sin^2\theta_{12}$, since $\sin^2\theta_{23}$ is almost fixed in these cases (see Fig. 2). Thus, the resulting likelihood profiles are not so broad in cases $A1A_5$ and $A2A_5$. In each case B (A), the value of the likelihood in the maximum is the same as in Fig. 1 (Fig. 2) as should be expected from the procedure of constructing the likelihood.

The dashed line in Fig. 3 stands for the likelihood extracted from the global analysis. More precisely, we take the one-dimensional projection $\chi^2_4(\delta)$ restricted to the interval of $\delta \in [180°, 360°]$ and translate it to $\chi^2_4(\cos\delta)$. Then, we use the latter to construct the likelihood. At present, all values of $\cos\delta$ are allowed at 3σ for NO, and almost all, $\cos\delta \in [-0.978, 0.995]$, for IO. We also show the dash-dotted and dotted lines, which represent two benchmark cases. The first case, marked in Fig. 3 as "Future 1" (the dash-dotted line), corresponds to the current best fit value $\delta^{\rm bf} = 234°(278°)$ for NO (IO) and the prospective 1σ uncertainty $\sigma(\delta) = 10°$. The second case, "Future 2" (the dotted line), corresponds to the potential best fit value $\delta^{\rm bf} = 270°$ (for both NO and IO) and the same error on δ of 10°. The corresponding χ^2 functions read

$$\chi^2_{4,\rm future}(\cos\delta) = \left(\frac{\cos\delta - \cos\delta^{\rm bf}}{\sigma(\cos\delta)}\right)^2, \qquad (4.6)$$

where $\sigma(\cos\delta)$ is obtained from $\sigma(\delta) = 10°$ using the derivative method of uncertainty propagation.

Finally, we perform statistical analysis of the predictions for $\cos\delta$ in cases C1, C3, C4, C8, $C3A_5$, and $C4A_5$. The corresponding correlations are given in Eqs. (2.9)–(2.12). Note that none of the mixing angles are predicted in these cases. We show the obtained likelihood functions for $\cos\delta$ in Fig. 4. As we see, all of them peak at values of $|\cos\delta| \sim 0.5$–1. There are two groups of cases: the first one consisting of C1, C3, and $C4A_5$ leads to negative values of $\cos\delta$, while the second one including C8 and $C3A_5$ predicts positive values. We find that case C4 is globally disfavored at more than 3σ, the corresponding $\chi^2_{\rm min}$ being 9.3 (13.6) for NO (IO). Therefore, we do not present this case in Fig. 4. On contrary, case $C4A_5$ is very well compatible with the data for NO, while for IO the compatibility is somewhat worse, at around 2σ. Case C3 reconciles with the data for NO (IO) at approximately 1.5σ (3σ). Case C1, being compatible at 2σ for NO, gets disfavored at more than 3σ for IO, the corresponding $\chi^2_{\rm min} = 12.7$. C8 is concordant with the data at almost 2σ (1.5σ) for NO (IO). Finally, the predictions of $C3A_5$ are compatible with the global data at 3σ.

Looking at the dotted line, we see that if in the future the best fit value of δ shifted to 270° and the LBL experiments managed to achieve the 1σ uncertainty on δ of 10°, cases C1, C3, and $C3A_5$ ($C4A_5$ and C8) would be disfavored at more than (at around) 3σ only by the measurement of δ. If, however, the current best fit value of δ for the NO spectrum is shown to be the true value for both the NO and IO spectra, cases $C3A_5$ and C8 will be ruled out by the

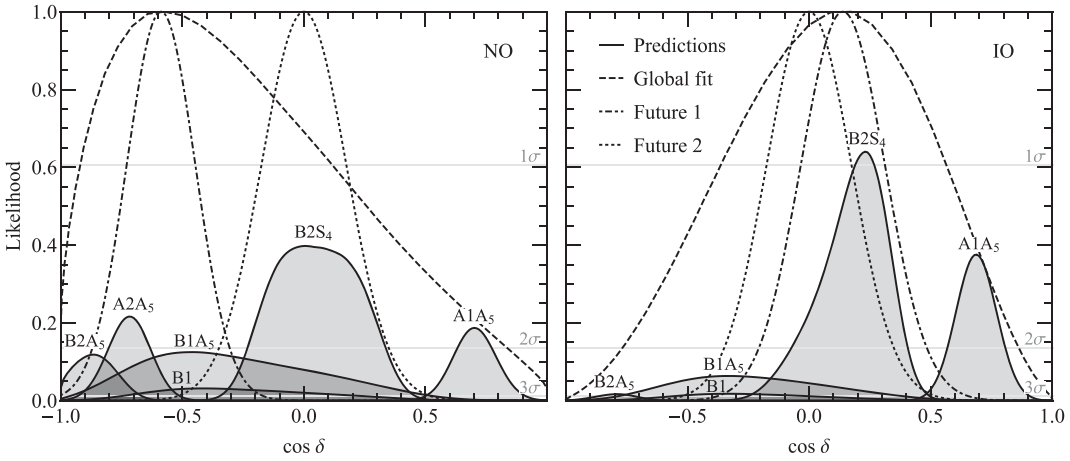

FIG. 3. Predictions for $\cos\delta$ in viable cases A and B obtained using the current global data on the neutrino mixing parameters. "Future 1" (the dash-dotted line) refers to the scenario with $\delta^{\rm bf} = 234°(278°)$ for NO (IO) (current best fit values) and the 1σ uncertainty on δ of 10°. "Future 2" (the dotted line) corresponds to $\delta^{\rm bf} = 270°$ and the 1σ uncertainty on δ of 10°. See text for further details.

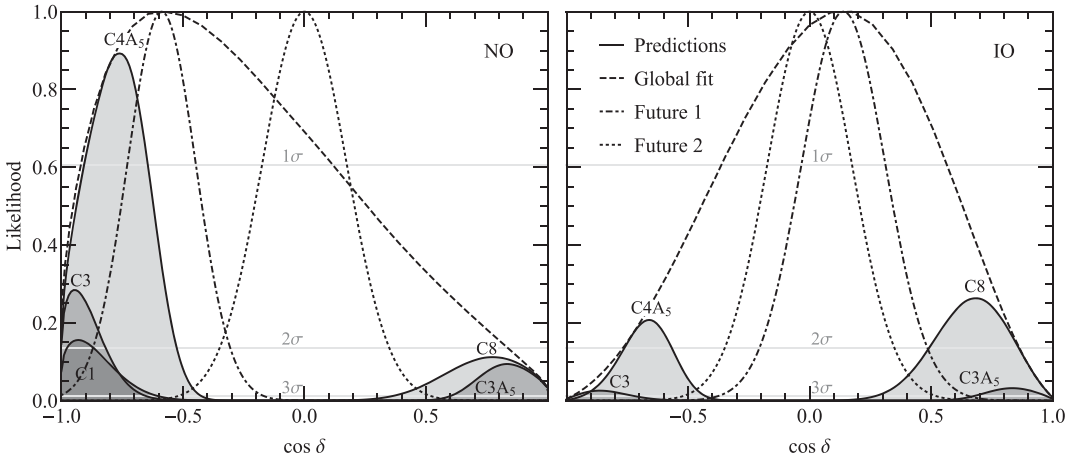

FIG. 4. The same as in Fig. 3, but for viable cases C.

measurement of δ with the indicated precision. In addition, the precision on $\sin^2\theta_{12}$ and $\sin^2\theta_{23}$ will be also improved. This will modify the likelihood profiles making them narrower. In the next section, we will study how this improvement will affect the results presented in Figs. 1–4.

C. Statistical analysis: Prospective data

In this section, we want to access the impact of the future precision measurements of the neutrino mixing angles on the predictions discussed in Sec. IV B. To this aim, we perform a statistical analysis of these predictions assuming that (i) the current best fit values of the mixing angles will not change in the future, and (ii) the prospective relative 1σ uncertainties on $\sin^2\theta_{12}$, $\sin^2\theta_{23}$, and $\sin^2\theta_{13}$ will amount to 0.7%, 3%, and 3%, respectively. As has already been mentioned, a measurement of $\sin^2\theta_{12}$ with such a high precision is expected from JUNO, while DUNE and T2HK will be able to reach 3% on $\sin^2\theta_{23}$ if atmospheric mixing deviates somewhat from maximal [see the discussion above Eq. (4.5)]. What concerns the reactor angle, Daya Bay is going to attain the precision of 3% on $\sin^2\theta_{13}$ by the year of 2020 [61]. The results of the analysis in this section should be considered only as indicative. Similar analysis should be performed when real data become available.

With these assumptions, we construct a global χ^2_{future} function as

$$\chi^2_{\text{future}}(\vec{y}) = \sum_{i=1}^{3} \chi^2_{i,\text{future}}(y_i), \tag{4.7}$$

where $\vec{y} = (\sin^2\theta_{12}, \sin^2\theta_{13}, \sin^2\theta_{23})$, the functions $\chi^2_{i,\text{future}}(y_i)$ with $i = 1$ and $i = 3$ are given in Eqs. (4.4) and (4.5), respectively, and we define $\chi^2_{2,\text{future}}(\sin^2\theta_{13})$ as

$$\chi^2_{2,\text{future}}(\sin^2\theta_{13}) = \left(\frac{\sin^2\theta_{13} - \sin^2\theta^{\text{bf}}_{13}}{\sigma(\sin^2\theta_{13})}\right)^2, \tag{4.8}$$

with $\sin^2\theta^{\text{bf}}_{13} = 0.02206(0.02227)$ being the current best fit value of $\sin^2\theta_{13}$ for NO (IO) and $\sigma(\sin^2\theta_{13}) = 0.03 \times \sin^2\theta^{\text{bf}}_{13}$ being the prospective 1σ uncertainty in its determination. We note that by constructing χ^2_{future} in this way, we do not assume any experimental input on δ. We use $\chi^2_{\text{future}}(\vec{y})$ instead of $\chi^2(\vec{x})$ in Eq. (4.2) to construct $\chi^2(\alpha)$. Finally, the likelihood function is calculated according to Eq. (4.3).

Cases predicting $\sin^2\theta_{12}$. As we have already mentioned earlier, it is clear from Fig. 1 that JUNO will be able to rule out all the cases predicting $\sin^2\theta_{12}$, if the best fit value of this parameter does not shift in the future (see the dotted line). However, this conclusion might change if the best fit value of $\sin^2\theta_{12}$ changes significantly.

Cases predicting $\sin^2\theta_{23}$. Since the predicted center value of $\sin^2\theta_{23} = 0.554$ in case A1A_5 matches exactly the current best fit value of this parameter for IO, this case will certainly survive in the future, if $\sin^2\theta^{\text{bf}}_{23}$ remains the same. Moreover, the precision on $\sin^2\theta_{23}$ is not expected to be as high as on $\sin^2\theta_{12}$, and we can infer from Fig. 2 that case C2S_4 has a chance to survive, while A2A_5 and C7S_4 do not. We have performed statistical analysis with the prospective uncertainties. The obtained results presented in Fig. 5 confirm our expectations. In particular, case A1A_5 would be perfectly compatible with the prospective data for IO. Note that now the amplitude of the likelihood profile is maximal, since we have not assumed any information on δ. For NO, the case under consideration would be slightly disfavored only due to the form of $\chi^2_{3,\text{future}}(\sin^2\theta_{23})$ (the dotted line). C2S_4 would be compatible at 2σ (3σ) with the prospective data for NO (IO), which is again dictated by the dotted line. For C7S_4, we find $\chi^2_{\text{min}} = 9.3(15.5)$ for NO (IO), and thus, we do not present this case in Fig. 5. The conclusions about the excluded cases should be revised if the best fit value of $\sin^2\theta_{23}$ shifts, e.g., to 0.5.

Cases predicting $\cos\delta$. Since all cases B as well as case A2A_5 would be ruled out by the prospective data we have

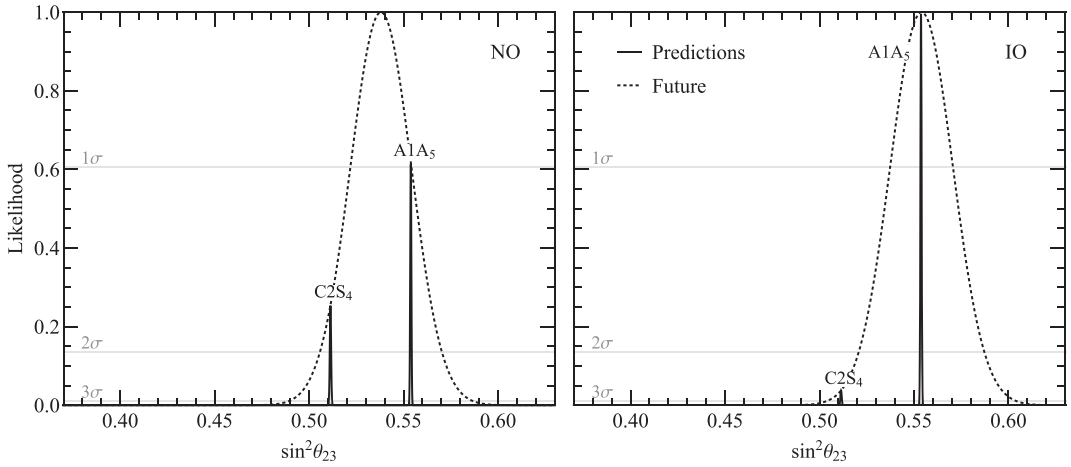

FIG. 5. Predictions for $\sin^2\theta_{23}$ obtained using the current best fit values and the prospective uncertainties in the determination of the neutrino mixing angles. "Future" (the dotted line) refers to the scenario with $\sin^2\theta_{23}^{\rm bf} = 0.538(0.554)$ for NO (IO) (current best fit values) and the relative 1σ uncertainty of 3% expected from DUNE and T2HK. See text for further details.

assumed, Fig. 3 would change significantly in the future, featuring *only* case $\mathrm{A1A_5}$. We present the likelihoods obtained in this case for NO and IO in Fig. 6. The width of the likelihood profiles in this figure is much smaller than that of the corresponding profiles in Fig. 3. This makes even more evident the fact that improving the precision on the mixing angles leads to sharper predictions for $\cos\delta$, which can and should be considered as an additional motivation of measuring the mixing angles with a high precision.

Finally, we perform statistical analysis of the predictions for $\cos\delta$ in cases C. We show the results in Fig. 7. We find that under the assumptions made case C1 would be ruled out. Thus, we would be left with four cases. Two of them lead to predictions which are in the corners of the parameter space for $\cos\delta$. Namely, C3 leads to values of $\cos\delta \lesssim -0.9(-0.8)$ for NO (IO), while $\mathrm{C3A_5}$ leads to $\cos\delta \gtrsim 0.9$. At least some of these values, if not all of them, will be ruled out by the future data on δ. In what concerns currently viable cases $\mathrm{C4A_5}$ and C8, they will be disfavored at approximately 3σ only by the measurement of δ if the true value of δ is indeed around 270° and the planned LBL experiments measure δ with a 1σ error of 10° (cf. Fig. 4). At the same time, if the current best fit value of δ for the NO spectrum turned out to be the true value for both the NO and IO spectra, cases C3 and $\mathrm{C4A_5}$ would "survive" this test. Thus, a high precision measurement of δ is crucial to firmly establish the status of the considered cases.

Before concluding, let us add two comments. First, the predictions considered in the present study can be tested simulating the future neutrino oscillation experiments, as it has been recently done, e.g., in Ref. [62], where DUNE and T2HK simulations have been performed to test the predictions for $\cos\delta$ of a setup [34] corresponding to pattern D

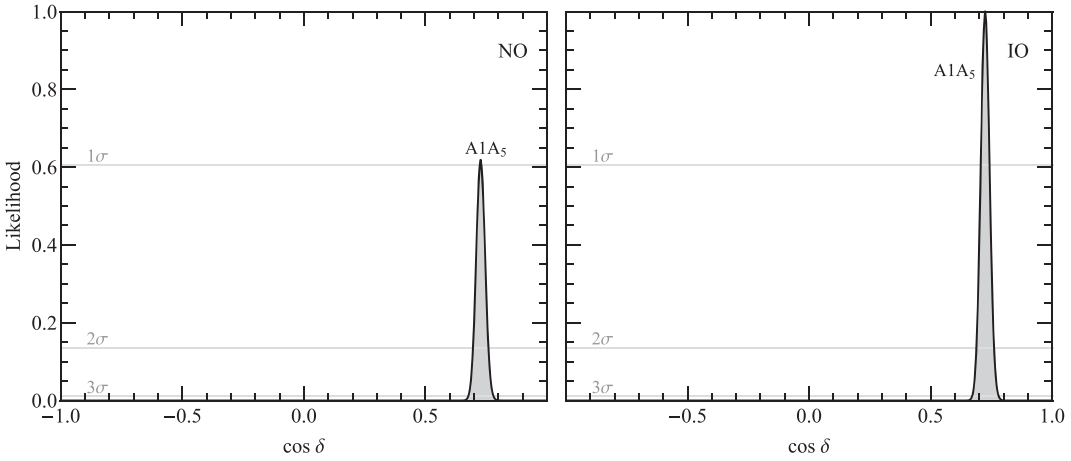

FIG. 6. Predictions for $\cos\delta$ in only viable case $\mathrm{A1A_5}$ obtained using the current best fit values and the prospective uncertainties in the determination of the neutrino mixing angles. See text for further details.

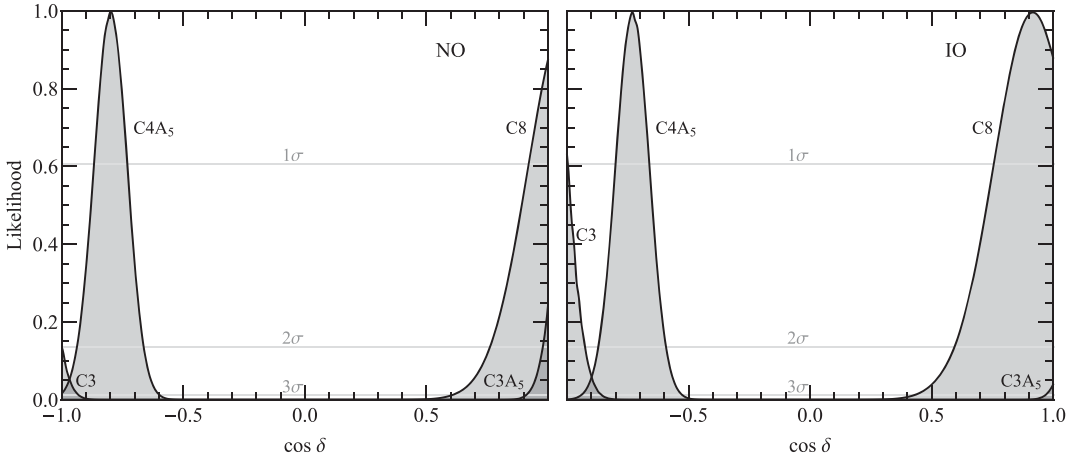

FIG. 7. The same as in Fig. 6, but for viable cases C.

of the discrete flavor symmetry breaking (see the Introduction). We plan to present such a study elsewhere. Secondly, it has been shown in Ref. [63] for a set of correlations arising in the same setup that renormalization group corrections to their predictions are negligible within the SM extended by the Weinberg dimension 5 operator to generate the neutrino masses, as well as in the MSSM with relatively small $\tan\beta$ and the lightest neutrino mass $\ll 0.01$ eV. The renormalization group corrections can be sizeable in the MSSM if these conditions are not fulfilled.

V. CONCLUSIONS

We have investigated the phenomenological viability of the discrete (lepton) flavor symmetries A_4, S_4, and A_5 for the description of neutrino mixing. More specifically, we have considered the A_4, S_4, and A_5 lepton flavor symmetry groups broken to nontrivial residual symmetry subgroups G_e and G_ν in the charged lepton and neutrino sectors. All flavor symmetry breaking patterns considered by us involve a Z_2 group as a residual symmetry in one of the two sectors, or two different Z_2 groups as residual symmetries in both sectors. More precisely, these patterns read: (A) $G_e = Z_2$ and $G_\nu = Z_k$, $k > 2$ or $Z_m \times Z_n$, $m, n \geq 2$; (B) $G_e = Z_k$, $k > 2$ or $Z_m \times Z_n$, $m, n \geq 2$, and $G_\nu = Z_2$; and (C) $G_e = Z_2$ and $G_\nu = Z_2$. In the cases corresponding to the pattern A (B) relations for $\sin^2\theta_{23}$ ($\sin^2\theta_{12}$) and $\cos\delta$ arise, while pattern C leads to constraints for either $\sin^2\theta_{12}$ or $\sin^2\theta_{23}$ or $\cos\delta$ [38], θ_{12}, θ_{23}, and δ being the solar, atmospheric neutrino mixing angles, and the Dirac CP violation phase of the PMNS neutrino mixing matrix.

We have performed a statistical analysis of the predictions for neutrino mixing parameters using as input the latest global neutrino oscillation data [49]. We have found 14 cases in total compatible with these data at 3σ confidence level. Five of them lead to very sharp predictions for $\sin^2\theta_{12}$ and four others to similarly sharp predictions for $\sin^2\theta_{23}$ (see Figs. 1 and 2). Phenomenologically viable cases A and B, which are six in total, lead as well to predictions for $\cos\delta$ presented in Fig. 3. Five viable C cases also lead to predictions for $\cos\delta$, which are summarized in Fig. 4. The corresponding likelihoods peak at values of $|\cos\delta| \sim 0.5$–1. As we have shown, the number of these cases could be further reduced by a sufficiently precise measurement of δ.

Further, we have performed a statistical analysis of the predictions discussed above assuming that (i) the current best fit values of the mixing angles will not change in the future, and (ii) the prospective relative 1σ uncertainties on $\sin^2\theta_{12}$, $\sin^2\theta_{23}$, and $\sin^2\theta_{13}$ will amount to 0.7%, 3%, and 3%, respectively. Such uncertainties are planned to be achieved by the JUNO, T2HK/DUNE, and Daya Bay experiments, respectively. Under the assumptions made, all the cases predicting $\sin^2\theta_{12}$ (see Fig. 1) get ruled out. In what concerns the cases predicting $\sin^2\theta_{23}$, two out of the four would "survive" this test (Fig. 5). We have found that only one case among six cases A and B viable at present would be compatible with the prospective data on the neutrino mixing angles. The predictions for $\cos\delta$ in this case are shown in Fig. 6. Four out of five cases C predicting $\cos\delta$ satisfy the expected constraints on the mixing angles. The corresponding predictions are summarized in Fig. 7. Thus, in total, six cases out of 14 viable at present are compatible with the assumed prospective data on the neutrino mixing angles, provided the current best fit values of the three neutrino mixing angles will not change drastically in the future. Five of these cases will be further critically tested by sufficiently precise data on the Dirac phase δ, e.g., if δ is measured with 1σ uncertainty of 10°. Obviously, the results obtained with the prospective data might change with the accumulation of new data if, e.g., the current best fit values of $\sin^2\theta_{12}$ and/or $\sin^2\theta_{23}$ change significantly.

In summary, we have shown that the A_4, S_4, and A_5 lepton flavor symmetries, broken to nontrivial residual

symmetries in the charged lepton and neutrino sectors, lead in the case of 3-neutrino mixing to a relatively small number of phenomenologically viable cases characterized by distinct predictions for the solar or atmospheric neutrino mixing angles θ_{12} and θ_{23} and/or for the cosine of the Dirac CP violation phase δ. We have also shown that the high precision measurements of the three neutrino mixing angles, planned to be performed by Daya Bay and the next generation of neutrino oscillation experiments—JUNO, T2HK, DUNE—can reduce the number of the phenomenologically viable cases to six. Five of these cases will be further critically tested by sufficiently precise data on the Dirac phase δ that could be provided by the T2HK and DUNE experiments.

The results obtained in the present study show that the future high precision data on the three neutrino mixing angles and on the leptonic Dirac CP violation phase δ, planned to be obtained in the Daya Bay, T2K, NOνA, and especially by the JUNO, T2HK, and DUNE experiments, will be crucial for testing the ideas of existence of new fundamental underlying discrete (non-Abelian) symmetry of the PMNS neutrino mixing matrix and of the lepton sector of particle physics.

ACKNOWLEDGMENTS

We would like to thank I. Girardi for the enjoyable collaboration on problems related to this work. This project received funding from the European Union's Horizon 2020 research and innovation program under the Marie Skłodowska-Curie Grants No. 674896 (ITN Elusives) and No. 690575 (RISE InvisiblesPlus). The work of S. T. P. was supported in part by the INFN program on Theoretical Astroparticle Physics (TASP) and by the World Premier International Research Center Initiative (WPI Initiative, MEXT), Japan. A. V. T. would like to thank Kavli IPMU for the hospitality and support during the final stages of the work on this project.

[1] C. D. Froggatt and H. B. Nielsen, Hierarchy of quark masses, Cabibbo angles and CP violation, Nucl. Phys. **B147**, 277 (1979).
[2] R. Barbieri and L. J. Hall, A grand unified supersymmetric theory of flavor, Nuovo Cimento Soc. Ital. Fis. A **110**, 1 (1997).
[3] R. Barbieri, L. J. Hall, S. Raby, and A. Romanino, Unified theories with U(2) flavor symmetry, Nucl. Phys. B **493**, 3 (1997).
[4] R. Barbieri, L. J. Hall, and A. Romanino, Consequences of a U(2) flavor symmetry, Phys. Lett. B **401**, 47 (1997).
[5] S. T. Petcov, On pseudo-Dirac neutrinos, neutrino oscillations and neutrinoless double beta decay, Phys. Lett. **110B**, 245 (1982).
[6] S. F. King and G. G. Ross, Fermion masses and mixing angles from SU (3) family symmetry and unification, Phys. Lett. B **574**, 239 (2003).
[7] G. Altarelli and F. Feruglio, Discrete flavor symmetries and models of neutrino mixing, Rev. Mod. Phys. **82**, 2701 (2010).
[8] H. Ishimori, T. Kobayashi, H. Ohki, Y. Shimizu, H. Okada, and M. Tanimoto, Non-Abelian discrete symmetries in particle physics, Prog. Theor. Phys. Suppl. **183**, 1 (2010).
[9] S. F. King and C. Luhn, Neutrino mass and mixing with discrete symmetry, Rep. Prog. Phys. **76**, 056201 (2013).
[10] I. Esteban, M. C. Gonzalez-Garcia, M. Maltoni, I. Martinez-Soler, and T. Schwetz, Updated fit to three neutrino mixing: Exploring the accelerator-reactor complementarity, J. High Energy Phys. 01 (2017) 087.
[11] F. Capozzi, E. Di Valentino, E. Lisi, A. Marrone, A. Melchiorri, and A. Palazzo, Global constraints on absolute neutrino masses and their ordering, Phys. Rev. D **95**, 096014 (2017).
[12] P. F. de Salas, D. V. Forero, C. A. Ternes, M. Tortola, and J. W. F. Valle, Status of neutrino oscillations 2017, Phys. Lett. B **782**, 633 (2018).
[13] C. S. Lam, Determining Horizontal Symmetry from Neutrino Mixing, Phys. Rev. Lett. **101**, 121602 (2008).
[14] C. Patrignani *et al.* (Particle Data Group Collaboration), Review of particle physics, Chin. Phys. C **40**, 100001 (2016).
[15] P. F. Harrison, D. H. Perkins, and W. G. Scott, Tri-bimaximal mixing and the neutrino oscillation data, Phys. Lett. B **530**, 167 (2002).
[16] P. F. Harrison and W. G. Scott, Symmetries and generalizations of tri-bimaximal neutrino mixing, Phys. Lett. B **535**, 163 (2002).
[17] Z.-z. Xing, Nearly tri bimaximal neutrino mixing and CP violation, Phys. Lett. B **533**, 85 (2002).
[18] X. G. He and A. Zee, Some simple mixing and mass matrices for neutrinos, Phys. Lett. B **560**, 87 (2003).
[19] L. Wolfenstein, Oscillations among three neutrino types and CP violation, Phys. Rev. D **18**, 958 (1978).
[20] F. Vissani, A study of the scenario with nearly degenerate Majorana neutrinos, arXiv:hep-ph/9708483.
[21] V. D. Barger, S. Pakvasa, T. J. Weiler, and K. Whisnant, Bimaximal mixing of three neutrinos, Phys. Lett. B **437**, 107 (1998).
[22] A. J. Baltz, A. S. Goldhaber, and M. Goldhaber, The Solar Neutrino Puzzle: An Oscillation Solution with Maximal Neutrino Mixing, Phys. Rev. Lett. **81**, 5730 (1998).
[23] G. Altarelli, F. Feruglio, and L. Merlo, Revisiting bimaximal neutrino mixing in a model with S_4 discrete symmetry, J. High Energy Phys. 05 (2009) 020.
[24] D. Meloni, Bimaximal mixing and large θ_{13} in a SUSY $SU(5)$ model based on S_4, J. High Energy Phys. 10 (2011) 010.

[25] G.-J. Ding and Y.-L. Zhou, Dirac neutrinos with S_4 flavor symmetry in warped extra dimensions, Nucl. Phys. B **876**, 418 (2013).

[26] A. Datta, F.-S. Ling, and P. Ramond, Correlated hierarchy, Dirac masses and large mixing angles, Nucl. Phys. B **671**, 383 (2003).

[27] Y. Kajiyama, M. Raidal, and A. Strumia, Golden ratio prediction for solar neutrino mixing, Phys. Rev. D **76**, 117301 (2007).

[28] L. L. Everett and A. J. Stuart, Icosahedral (A_5) family symmetry and the golden ratio prediction for solar neutrino mixing, Phys. Rev. D **79**, 085005 (2009).

[29] G.-J. Ding, L. L. Everett, and A. J. Stuart, Golden ratio neutrino mixing and A_5 flavor symmetry, Nucl. Phys. B **857**, 219 (2012).

[30] W. Rodejohann, Unified parametrization for quark and lepton mixing angles, Phys. Lett. B **671**, 267 (2009).

[31] A. Adulpravitchai, A. Blum, and W. Rodejohann, Golden ratio prediction for solar neutrino mixing, New J. Phys. **11**, 063026 (2009).

[32] C. H. Albright, A. Dueck, and W. Rodejohann, Possible alternatives to tri-bimaximal mixing, Eur. Phys. J. C **70**, 1099 (2010).

[33] J. E. Kim and M.-S. Seo, Quark and lepton mixing angles with a dodeca-symmetry, J. High Energy Phys. 02 (2011) 097.

[34] S. T. Petcov, Predicting the values of the leptonic *CP* violation phases in theories with discrete flavour symmetries, Nucl. Phys. B **892**, 400 (2015).

[35] I. Girardi, S. T. Petcov, and A. V. Titov, Predictions for the leptonic Dirac *CP* violation phase: A systematic phenomenological analysis, Eur. Phys. J. C **75**, 345 (2015).

[36] W. Grimus and L. Lavoura, A model for trimaximal lepton mixing, J. High Energy Phys. 09 (2008) 106.

[37] C. H. Albright and W. Rodejohann, Comparing trimaximal mixing and its variants with deviations from tri-bimaximal mixing, Eur. Phys. J. C **62**, 599 (2009).

[38] I. Girardi, S. T. Petcov, A. J. Stuart, and A. V. Titov, Leptonic Dirac *CP* violation predictions from residual discrete symmetries, Nucl. Phys. B **902**, 1 (2016).

[39] S. T. Petcov, Discrete flavour symmetries, neutrino mixing and leptonic *CP* violation, arXiv:1711.10806.

[40] D. Marzocca, S. T. Petcov, A. Romanino, and M. C. Sevilla, Nonzero $|U_{e3}|$ from charged lepton corrections and the atmospheric neutrino mixing angle, J. High Energy Phys. 05 (2013) 073.

[41] I. Girardi, S. T. Petcov, and A. V. Titov, Determining the Dirac *CP* violation phase in the neutrino mixing matrix from sum rules, Nucl. Phys. B **894**, 733 (2015).

[42] A. Meroni, S. T. Petcov, and M. Spinrath, A supersymmetric $SU(5) \times T'$ unified model of flavour with large θ_{13}, Phys. Rev. D **86**, 113003 (2012).

[43] C. Hagedorn and D. Meloni, D_{14}—A common origin of the Cabibbo angle and the lepton mixing angle θ_{13}^l, Nucl. Phys. B **862**, 691 (2012).

[44] S. Antusch, C. Gross, V. Maurer, and C. Sluka, A flavour GUT model with $\theta_{13}^{\mathrm{PMNS}} \simeq \theta_C/\sqrt{2}$, Nucl. Phys. B **877**, 772 (2013).

[45] M.-C. Chen, J. Huang, K. T. Mahanthappa, and A. M. Wijangco, Large θ_{13} in a SUSY $SU(5) \times T'$ model, J. High Energy Phys. 10 (2013) 112.

[46] I. Girardi, A. Meroni, S. T. Petcov, and M. Spinrath, Generalised geometrical *CP* violation in a T' lepton flavour model, J. High Energy Phys. 02 (2014) 050.

[47] J. Gehrlein, J. P. Oppermann, D. Schfer, and M. Spinrath, An $\mathrm{SU}(5) \times \mathrm{A}_5$ golden ratio flavour model, Nucl. Phys. B **890**, 539 (2014).

[48] F. Feruglio, C. Hagedorn, Y. Lin, and L. Merlo, Tri-bimaximal neutrino mixing and quark masses from a discrete flavour symmetry, Nucl. Phys. B **775**, 120 (2007); Erratum, Nucl. Phys. B **836**, 127 (2010).

[49] I. Esteban, M. C. Gonzalez-Garcia, A. Hernandez-Cabezudo, M. Maltoni, I. Martinez-Soler, and T. Schwetz, NuFIT 3.2: Three-neutrino fit based on data available in January 2018, www.nu-fit.org.

[50] M. Tanimoto, Neutrinos and flavor symmetries, AIP Conf. Proc. **1666**, 120002 (2015).

[51] F. Feruglio, C. Hagedorn, and R. Ziegler, Lepton mixing parameters from discrete and *CP* symmetries, J. High Energy Phys. 07 (2013) 027.

[52] G.-J. Ding, S. F. King, and A. J. Stuart, Generalised *CP* and A_4 family symmetry, J. High Energy Phys. 12 (2013) 006.

[53] J. T. Penedo, S. T. Petcov, and A. V. Titov, Neutrino mixing and leptonic *CP* violation from S_4 flavour and generalised *CP* symmetries, J. High Energy Phys. 12 (2017) 022.

[54] I. Girardi, S. T. Petcov, and A. V. Titov, Predictions for the Dirac *CP* violation phase in the neutrino mixing matrix, Int. J. Mod. Phys. A **30**, 1530035 (2015).

[55] F. An *et al.* (JUNO Collaboration), Neutrino physics with JUNO, J. Phys. G **43**, 030401 (2016).

[56] R. Acciarri *et al.*, DUNE Collaboration, Long-Baseline Neutrino Facility (LBNF) and Deep Underground Neutrino Experiment (DUNE) conceptual design report, volume 1: The LBNF and DUNE projects, arXiv:1601.05471.

[57] R. Acciarri *et al.* (DUNE Collaboration), Long-Baseline Neutrino Facility (LBNF) and Deep Underground Neutrino Experiment (DUNE) conceptual design report, volume 2: The physics program for DUNE at LBNF, arXiv:1512.06148.

[58] K. Abe *et al.* (Hyper-Kamiokande Working Group Collaboration), A long baseline neutrino oscillation experiment using J-PARC neutrino beam and Hyper-Kamiokande, arXiv:1412.4673.

[59] K. Abe *et al.* (Hyper-Kamiokande Proto Collaboration), Physics potential of a long-baseline neutrino oscillation experiment using a J-PARC neutrino beam and Hyper-Kamiokande, Prog. Theor. Exp. Phys. **2015**, 053C02 (2015).

[60] P. Ballett, S. F. King, S. Pascoli, N. W. Prouse, and T. Wang, Sensitivities and synergies of DUNE and T2HK, Phys. Rev. D **96**, 033003 (2017).

[61] J. Ling (Daya Bay Collaboration), Precision measurement of $\sin^2(2\theta_{13})$ and $|\Delta m^2_{ee}|$ from Daya Bay, Proc. Sci. ICHEP2016 (2016) 467.

[62] S. K. Agarwalla, S. S. Chatterjee, S. T. Petcov, and A. V. Titov, Addressing neutrino mixing models with DUNE and T2HK, Eur. Phys. J. C **78**, 286 (2018).

[63] J. Gehrlein, S. T. Petcov, M. Spinrath, and A. V. Titov, Renormalisation group corrections to neutrino mixing sum rules, J. High Energy Phys. 11 (2016) 146.